is orange, gives green solutions under similar conditions. As with some other properties of the systems, these differences are puzzling and deserve further study.

**Acknowledgment.** We thank the Robert A. Welch Foundation for support under Grant No. A-494.

**Registry No.** *cis*-$TaCl_4(PMe_2Ph)_2$, 92763-08-1; $TaCl_4(PMe_3)_3$, 92763-09-2; *trans*-$TaCl_4(PEt_3)_2$, 73079-36-4.

**Supplementary Material Available:** Tables of structure factors and anisotropic thermal parameters ($B$'s) and full listings of bond distances and angles for all three compounds (37 pages). Ordering information is given on any current masthead page.

---

Contribution from the Departments of Chemistry, University of Alabama, University, Alabama 35486, and University of Victoria, Victoria, British Columbia, Canada V8W 2Y2

# Pyrazolyl-Bridged Iridium Dimers. 6.[1] Two-Fragment, Two-Center Oxidative Addition of Halogens and Methyl Halides to *trans*-Bis(triphenylphosphine)dicarbonylbis(μ-pyrazolyl)diiridium(I)

JERRY L. ATWOOD,[†] KATHY A. BEVERIDGE,[‡] GORDON W. BUSHNELL,[‡] KEITH R. DIXON,[‡]
DONALD T. EADIE,[‡] STEPHEN R. STOBART,*[‡] and MICHAEL J. ZAWOROTKO[†]

*Received February 8, 1983*

Reaction between *trans*-$Ir(PPh_3)_2(CO)Cl$ and Na(pz) (pzH = $C_3N_2H_4$, pyrazole) affords the scarlet diiridium complex $[Ir(PPh_3)(CO)(\mu\text{-pz})]_2$ (**1a**) characterized by single-crystal X-ray crystallography, in which the terminal $PPh_3$ and CO ligands are mutually trans across the $Ir_2$ axis with a formally nonbonded $Ir_2$ separation of 3.163 (2) Å; the latter is somewhat longer [3.290 (1) Å] in the orange-red hexane solvate (**1b**). A systematic synthesis of the same compound is described, in which reaction of $[Ir(COD)Cl]_2$ with pzH giving the dimer $[Ir(COD)(\mu\text{-pz})]_2$ (**2**) is followed by treatment with CO and $PPh_3$ to provide **1** in 82% yield. Reaction of **1** with $Ir_2$ and $Br_2$ leads to formation of yellow complexes formulated as 1:1 adducts formed by a two-center oxidative addition, i.e. $[Ir(PPh_3)(CO)(X)(\mu\text{-pz})]_2$ (X = I, Br); with $Cl_2$ the corresponding product has been characterized crystallographically as $[Ir(PPh_3)(CO)(Cl)(4\text{-Cl-pz})]_2$ (**9**) in which the trans configuration of **1** is retained. Axial substitution at each Ir with Ir–Cl = 2.443 (6) Å has been accompanied by formation of a metal–metal bond [Ir–Ir = 2.737 (1) Å] and electrophilic substitution by Cl of the 4-position in each bridging pyrazolyl-ring system. Reaction between **1** and MeI affords a yellow 1:1 adduct (80% yield) for which a corresponding dimeric structure is proposed having Me attached to Ir(1) and I to Ir(2); by contrast with MeBr, reaction is slower to give an unidentified mixture of products. Crystals of **1a** are triclinic, space group $P\bar{1}$: $a = 9.992$ (4), $b = 10.402$ (4), $c = 20.278$ (8) Å; $\alpha = 90.01$ (4), $\beta = 90.10$ (4), $\gamma = 105.13$ (4)°. Modification **1b** crystallizes in $P2_1/c$: $a = 15.528$ (4), $b = 9.713$ (3), $c = 30.544$ (8) Å; $\beta = 93.98$ (2)°. For the addition product (**9**), the space group is $P2_1/n$: $a = 15.851$ (3), $b = 28.617$ (4), $c = 11.092$ (2) Å; $\beta = 95.82$ (2)°.

## Introduction

Oxidative-addition reactions have been extensively studied as models for those homogeneous metal-assisted catalytic transformations of organic substrates in which successive alternation with the reverse process, i.e. a reductive-elimination step, is thought to be instrumental in establishing a continuous cycle. Where such circumstances lead to effective catalysis, the metal complexes participating as reactive intermediates may be so labile or present in such low concentration that proper characterization of these species becomes problematic. In other examples of reactions involving oxidative addition, kinetically stable adducts have been obtained that are amenable to structural identification, establishing coordination geometries that by analogy have been projected to transient reactive configurations. A by now classical illustration of this kind of correlation is provided by the difference in properties between six-coordinate *cis*-dihydrido complexes of rhodium and iridium: while examples of the latter have been characterized in the solid state as typical octahedral Ir(III) derivatives,[2] the former are generated only reversibly,[3] in the crucial step of the catalytic hydrogenation of unsaturated compounds by $RhCl(PPh_3)_3$. Only much more recently however, has it become apparent that oxidative addition may result in attachment of substrate fragments at other than a single metal site, although such events have frequently been hypothesized in relation to cooperativity effects in biological systems as well as in the context of heterogeneous catalytic reactions, especially reorganization of organic molecules at metal surfaces.

In 1975 the addition of $CH_3I$ to $Au_2[(CH_2)_2PMe_2]_2$ was claimed by Schmidbaur and Franke,[4] and in the following year isolation of methyl halide adducts of the binuclear cation $Rh_2[CN(CH_2)_3NC]_4^{2+}$ was reported by Gray et al.[5] In both cases reaction was taken to result in metal–metal bond formation as represented generally by eq 1, i.e. with a unit in-

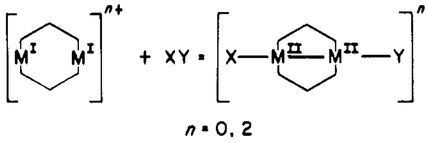

(1)

crease in the formal oxidation number of each metal center

---

[†] University of Alabama.

[‡] University of Victoria.

(1) (a) Part 2: Coleman, A. W.; Eadie, D. T.; Stobart, S. R.; Zaworotko, M. J.; Atwood, J. L. *J. Am. Chem. Soc.* **1982**, *104*, 922. (b) Part 3: Bushnell, G. W.; Fjeldsted, D. O. K.; Stobart, S. R.; Zaworotko, M. J. *J. Chem. Soc., Chem. Commun.* **1983**, 580. (c) Part 4: Beveridge, K. A.; Bushnell, G. W.; Stobart, S. R.; Atwood, J. L.; Zaworotko, M. J. *Organometallics* **1983**, *2*, 1447. (d) Part 5: Bushnell, G. W.; Stobart, S. R.; Vefghi, R.; Zaworotko, M. J. *J. Chem. Soc., Chem. Commun.* **1984**, 282.

(2) Hyde, E. M.; Shaw, B. L. *J. Chem. Soc., Dalton Trans.* **1975**, 765. Vaska, L. *Acc. Chem. Res.* **1968**, *1*, 335. Halpern, J. *Ibid.* **1979**, *3*, 386. See also: Longato, B.; Morandini, F.; Bresadola, S. *Inorg. Chem.* **1976**, *15*, 650.

(3) Osborn, J. A.; Jardine, F. H.; Young, J. F.; Wilkinson, G. *J. Chem. Soc. A* **1966**, 1711. Tolman, C. A.; Meakin, P. Z.; Lindner, D. L.; Jesson, J. P. *J. Am. Chem. Soc.* **1974**, *96*, 2762.

(4) Schmidbaur, H.; Franke, R. *Inorg. Chem. Acta* **1975**, *13*, 85. Very recently the product of this addition has been characterized crystallographically, showing Au(1)–C = 2.13 (5), Au(2)–I = 2.894 (5), and Au(1)–Au(2) = 2.695 (4) Å: Fackler, J. P.; Basil, J. D. *Organometallics* **1982**, *1*, 871.

(5) Lewis, N. S.; Mann, K. R.; Gordon, J. G.; Gray, H. B. *J. Am. Chem. Soc.* **1976**, *98*, 7461.

0020-1669/84/1323-4050$01.50/0

via attachment at each of a substrate fragment. To date only a small number of further examples paralleling this behavior have been described, as noted very recently by Balch[6] in introducing the novel three-fragment, two-center addition of organic dihalides expressed as eq 2.

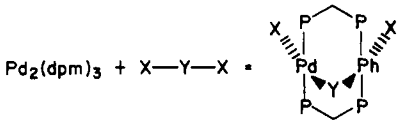

(2)

Our activity in this area began in 1979, when it was found that reaction of sodium pyrazolide (Na(pz))[7] with *trans*-Ir$(PPh_3)_2(CO)Cl$ ("Vaska's complex") affords a dimeric product $[Ir(PPh_3)(CO)(\mu\text{-pz})]_2$ (**1**) and that addition to this complex of halogens or methyl iodide occurs under mild conditions.[8] Subsequently, a systematic route to compound **1** as well as analogues incorporating alternate pyrazolyl bridging ligands or terminal tertiary phosphines was developed, proceeding via $[(COD)Ir(\mu\text{-pz})]_2$ (**2**) (COD = cycloocta-1,5-diene); it was discovered[7] also that this latter diiridium system can itself enter into facile and reversible[9] addition reactions. The rhodium analogues of **1** and **2** are known: the synthesis of $[Rh(PPh_3)(CO)(\mu\text{-pz})]_2$ (**3**) was reported[10] in 1981 through successive reaction with CO then $PPh_3$ of $[(COD)Rh(\mu\text{-pz})]_2$ (**4**), which was first prepared a number of years ago by Trofimenko.[11] Although no oxidative-addition reactions corresponding to those we have described[8,9] have been observed for **3** or **4**, similar chemistry is characteristic of another dimeric iridium system $[Ir(PR_3)(CO)(\mu\text{-}t\text{-BuS})]_2$ (**5**; R = OMe) to which will add dihdyrogen[12] or diiodine.[13] Finally and most recently, oxidation of $[Ir(PR_3)(CO)(\mu\text{-3,5-dmp})]_2$ (**6**; R = OPh, dmp = dimethylpyrazolyl) by $I_2$ or 1,2-diiodoethane paralleling that[8,9] of **1** or **2** has been communicated.[14]

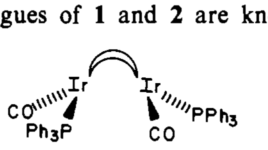

**1**

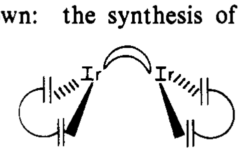

**2**

In this paper we discuss the characterization by X-ray crystallography of the pyrazolyl-bridged iridium(I) dimer (**1**) and its reactions with halogens and with methyl iodide, which give adducts formulated as the products of a two-center oxidative addition. We have established unequivocally that dichlorine addition to **1** does proceed according to eq 1: determination by X-ray methods of the structure of the oxidized molecule reveals that the Ir–Ir separation has indeed shortened to within bonding distance. Formation of a metal–metal bond in this way (see eq 1) represents a classical ("Wernerian") response of a binuclear metal complex to oxidative addition, the opposite of that demonstrated by multiply bonded analogues for which identical chemistry occurs with a reduction in bond order.[15,16]

## Experimental Section

**(a) General Procedures.** All operations were conducted under an atmosphere of dry dinitrogen gas with standard Schlenk techniques, and solvents were carefully dried and redistilled before use. IR spectra were obtained on a Perkin-Elmer 283 spectrophotometer, and NMR spectra were measured on Perkin-Elmer R32 (90 MHz, $^1H$) or Nicolet TT14 (15.1 MHz, $^{13}C$; 24.3 MHz, $^{31}P$) instruments. Microanalyses were performed by Canadian Microanalytical Services Ltd. Pyrazole was used as supplied (Aldrich Chemical Co.); $IrCl_3 \cdot 3H_2O$ was supplied by Johnson-Matthey Inc.

**(b) Bis(triphenylphosphine)dicarbonylbis($\mu$-pyrazolyl)diiridium(I), $[Ir(CO)(PPh_3)_2(\mu\text{-pz})]_2$ (1). Method A.** A filtered solution of sodium pyrazolide, $NaC_3N_2H_3$ in THF (20 $cm^3$), prepared by stirring $C_3N_2H_4$ (0.045 g, 0.79 mmol) and NaH (0.022 g, 0.91 mmol) for 2 h at ambient temperature, was added slowly to a solution of *trans*-$IrCl(CO)(PPh_3)_2$ (0.3 g, 0.38 mmol) in THF (30 $cm^3$). An orange color developed during stirring at 25 °C (5 h), and on removal of THF an orange oil remained that was washed with hexane (5 × 10 $cm^3$). Dissolution in THF (20 $cm^3$) was followed by filtration and concentration to ca. 6-$cm^3$ volume, after which hexane (15 $cm^3$) was run in to form an upper layer. Refrigeration afforded the product as deep red needles or orange crystals, yield typically 0.25 g (60%). Anal. Calcd for $C_{44}H_{36}Ir_2N_4O_2P_2$: C, 48.1; H, 3.32; N, 5.10. Found: C, 49.2; H, 3.38; N, 5.03.

**Method B.** Into an orange-red, stirred solution of $[Ir(C_8H_{12})Cl]_2$ (0.095 g, 0.14 mmol; $C_8H_{12}$ = COD, prepared by published procedures) in THF (10 $cm^3$) was added dropwise a mixture of pyrazole (pzH; 0.02 g, 0.28 mmol) and $NEt_3$ (0.1 $cm^3$, 0.7 mmol) in THF (10 $cm^3$). The color of the reaction mixture rapidly became deep purple-red, and after 0.5 h, the solvent was removed and the residue was pumped to dryness (1 h, $10^{-2}$ mmHg). Extraction with THF (35 $cm^3$), filtration through neutral alumina (15 g), and concentration to 5 $cm^3$ was followed by dropwise addition of hexane (10 $cm^3$); refrigeration (−28 ° C, 24 h) afforded $[(COD)Ir(\mu\text{-pz})]_2$ (**2**) as deep red needles, yield 0.097 g (93%). Anal. Calcd for $C_{22}H_{30}Ir_2N_4$: C, 35.9; H, 4.11; N, 7.62. Found: C, 35.8; H, 4.11; N, 7.26. When a stream of CO was bubbled through a solution of complex **2** (0.12 g, 0.16 mmol) in THF (50 $cm^3$), the color quickly became light orange-yellow. Removal of solvent at this point resulted in spontaneous deposition of black, insoluble material, but addition of $PPh_3$ (0.086 g, 0.32 mmol) in hexane (10 $cm^3$) afforded a rapid color change to orange-red and gas evolution occurred. After 15 min the solution was concentrated to 15 $cm^3$, and hexane (25 $cm^3$) was added as an upper layer. The product (yield 0.13 g (82%)) formed orange or scarlet crystals shown to be identical with that obtained by method A.

**(c) Reactions of Complex 1 with Halogens. With Diiodine.** To a solution of compound **1** (0.117 g, 0.106 mmol) in 2:1 $Et_2O$/THF (15 $cm^3$) was added dropwise with stirring at 25 °C a solution of $I_2$ (0.027 g, 0.106 mmol) in $Et_2O$ (12 $cm^3$). This resulted in rapid precipitation of a bright yellow powder, which was recovered after a reaction time of 0.5 h. Thorough washing with hexane (6 × 5 $cm^3$) followed by drying in vacuo yielded the dark yellow product, $[Ir(PPh_3)(CO)(I)(\mu\text{-pz})]_2$ (**7**), yield 0.12 g (84%). Anal. Calcd for $C_{44}H_{36}I_2Ir_2N_4O_2P_2$: C, 39.0; H, 2.68; N, 4.14. Found: C, 38.4; H, 2.73; N, 4.02.

**With Dibromine.** Compound **1** (0.057 g, 0.052 mmol) in $Et_2O$ (20 $cm^3$) and THF (5 $cm^3$) was treated with $Br_2$ (1 equiv, 0.27 $cm^3$) in $Et_2O$ (20 $cm^3$); the solution rapidly changed from deep orange to yellow, and a bright yellow solid was deposited. This was collected, washed with hexane, (2 × 10 $cm^3$), and dried to give 0.05 g (70%) of the yellow product, $[Ir(PPh_3)(CO)(Br)(\mu\text{-pz})]_2$ (**8**). Anal. Calcd for $C_{44}H_{36}Br_2Ir_2N_4O_2P_2$: C, 41.9; H, 2.88; N, 4.45. Found: C, 41.2; H, 2.80; N, 4.40.

**With Dichlorine.** When dry $Cl_2$ gas was bubbled into a solution in THF (30 $cm^3$) of complex **1** (0.10 g, 0.091 mmol), an instant color change occurred from orange-red to pale yellow. Concentration to 8 $cm^3$ followed by standing at 0 °C for 24 h afforded the product as hexagonal yellow plates, yield 0.08 g (72%); recrystallization from $CH_2Cl_2$ yielded yellow needles of the bis(methylene chloride) solvate of *dicarbonyldichlorobis(triphenylphosphine)bis($\mu$-4-chloropyrazolyl)diiridium(II)* (**9**). Anal. Calcd for $C_{46}H_{38}Cl_4Ir_2N_4O_2P_2$: C, 39.2; H, 2.70; N, 3.98. Found: C, 39.8; H, 2.54; N, 3.96.

---

(6) Balch, A. L.; Hunt, C. T.; Lee, C.-L.; Olmstead, M. M.; Farr, J. P. *J. Am. Chem. Soc.* **1981**, *103*, 3764.

(7) Throughout this paper: pzH = pyrazole; pz = pyrazolyl; dpz = 3,5-dimethylpyrazolyl.

(8) Beveridge, K. A.; Bushnell, G. W.; Dixon, K. R.; Eadie, D. T.; Stobart, S. R.; Atwood, J. L.; Zaworotko, M. J. *J. Am. Chem. Soc.* **1982**, *104*, 920.

(9) Coleman, A. W.; Stobart, S. R., unpublished observations.

(10) Uson, R.; Oro, L. A.; Ciriano, M. A.; Pinillos, M. T.; Tiripicchio, A.; Tiripicchio Camellini, M. *J. Organomet. Chem.* **1981**, *205*, 247.

(11) Trofimenko, S. *Inorg. Chem.* **1971**, *10*, 1372.

(12) Bonnet, J. J.; Thorez, A.; Maissonat, A.; Galy, J.; Poilblanc, R. *J. Am. Chem. Soc.* **1979**, *101*, 5940.

(13) Bonnet, J. J.; Kalck, P.; Poilblanc, R. *Angew. Chem., Int. Ed. Engl.* **1980**, *19*, 551.

(14) Powell, J.; Kuksis, A.; Nyburg, S. C.; Ng, W. W. *Inorg. Chim. Acta* **1982**, *64*, L211.

(15) Chisholm, M. H.; Kirkpatrick, C. C.; Huffman, J. C. *Inorg. Chem.* **1981**, *20*, 871.

(16) Cotton, F. A.; Chisholm, M. H. *Chem. Eng. News* **1982**, *60* (June 28), 40.

Table I. Crystal Data and Summary of Intensity Data Collection and Structure Refinement for 1a, 1b, and 9

| | $[Ir(PPh_3)(CO)(\mu\text{-pz})]_2$ | $[Ir(PPh_3)(CO)(\mu\text{-pz})]_2$ $(C_6H_{14})$ | $[Ir(PPh_3)(CO)Cl(\mu\text{-pz})]_2$ $(2CH_2Cl_2)$ |
|---|---|---|---|
| mol wt | 1099.1 | 1185.3 | 1408.8 |
| cell dimens | | | |
| *a*, Å | 9.992 (4) | 15.528 (4) | 15.851 (3) |
| *b*, Å | 10.402 (4) | 9.713 (3) | 28.617 (4) |
| *c*, Å | 20.278 (8) | 30.544 (8) | 11.092 (2) |
| α, deg | 90.01 (4) | 90. | 90. |
| β, deg | 90.10 (4) | 93.98 (2) | 95.82 (2) |
| γ, deg | 105.13 (4) | 90. | 90. |
| *V*, Å$^3$ | 2037 | 4595 | 5005 |
| *Z* | 2 | 4 | 4 |
| $\rho_{calcd}$, g cm$^{-3}$ | 1.79 | 1.71 | 1.869 |
| $\mu_{calcd}$, cm$^{-1}$ (Mo Kα) | 63.8 | 62.4 | 61.7 |
| max cryst dimens, mm | 0.05 × 0.05 × 0.20 | 0.05 × 0.10 × 0.20 | *a* |
| scan width (θ) | 0.80 + 0.20 tan θ | 0.80 + 0.20 tan θ | 1.00 |
| decay of stds | ±2% | ±2% | ±18% |
| 2θ range, deg | 4–36 | 4–36 | 2–40 |
| no. of obsd reflcns | 1481 | 2611 | 3003 |
| no. of parameters varied | 237 | 255 | 577 |
| *R* | 0.046 | 0.055 | 0.050 |
| $R_w$ | 0.055 | 0.062 | 0.051 |
| space group | $P\bar{1}$ | $P2_1/c$ | $P2_1/n$ |

[a] Crystal face indices and perpendicular distances to the origin (mm): pinakoidal forms {010}, 0.082; {100}, 0.265; {101}, 0.131; {1,0,–1}, 0.299; {111}, 0.128.

**(d) Reactions of Complex 1 with Methyl Iodide and with Methyl Bromide.** To a stirred solution in THF (30 cm$^3$) of complex **1** (0.11 g, 0.10 mmol) was added dropwise over 2 min MeI (1 equiv, 0.62 cm$^3$ of a solution of 0.5 cm$^3$ in 50 cm$^3$ of $Et_2O$). Concentration to 5 cm$^3$ followed by addition of hexane (5 cm$^3$) and slow cooling to –25 °C afforded the product, $[Ir_2(PPh_3)_2(CO)_2(\mu\text{-pz})_2(Me)(I)]$ (**10**) as a yellow powder, yield 0.10 g (80%). Anal. Calcd for $C_{45}H_{39}IIr_2N_4O_2P_2$: C, 41.7; H, 3.17; N, 4.51. Found: C, 42.2; H, 3.13; N, 4.18. An identical product was obtained from reaction of complex **1** with excess MeI. Treatment of **1** with MeBr under similar conditions led to a slower (12-h) lightening of the reaction mixture to pale yellow; IR and $^{31}P$ NMR spectroscopy were consistent with the presence of more than one product, and attempts to isolate a bromo analogue of compound **10** have so far been unsuccessful.

**(e) X-ray Data Collection and Structure Refinement. Compounds 1a and 1b.** Crystallization of complex **1** as blood red needles (**1a**) or orange-red plates (**1b**) suggested the possible existence of configurational isomers, but crystallographic analysis has demonstrated (see Results and Discussion) that these are unsolvated and solvated forms of *trans*-$[Ir(PPh_3)(CO)(\mu\text{-pz})]_2$, respectively. Final lattice parameters for **1a** and **1b**, as determined from least-squares refinements of the angular settings of 15 reflections (2θ > 30°) accurately centered on an Enraf-Nonius CAD-4 diffractometer, are given along with other pertinent crystallographic parameters in Table I. Following correction for Lorentz, polarization, and absorption effects, both structures were solved via application of the direct-methods program MULTAN.[17] Subsequent least-squares refinements were carried out with the SHELX program package.[18] With iridium and phosphorus atoms only refined with anisotropic thermal parameters, final values of $R = [\sum(|F_o| - |F_c|)/\sum|F_o|] = 0.046$ and 0.055 and $R_w = [\sum w(|F_o| - |F_c|)^2/\sum F_o^2]^{1/2} = 0.055$ and 0.062 were obtained for **1a** and **1b**, respectively. Hydrogen atoms were not locatable in either compound. Neutral-atom scattering factors were taken from the compilations of Cromer and Mann,[19] and corrections for the real and imaginary components of anomalous dispersion were taken from the table of Cromer and Liberman.[20] Final fractional atomic coordinates are given in Tables II and III for **1a** and **1b**, respectively.

At a later date compound **1b** was again examined with the aim of obtaining a more complete data set. This time, data were collected to 2θ = 50°, and 3316 were considered observed (*I* > 3σ(*I*)). Refinement led to *R* = 0.082, with only the Ir and P atoms refined with anisotropic thermal parameters. One of the N atoms refined to an unrealistic temperature factor (not positive definite) upon attempted refinement of the lighter atoms with anisotropic thermal parameters. Thus, it was not possible to obtain a better refinement than that reported in Table III. This exercise did verify the Ir···Ir contact: the second refinement gave a value of 3.294 (2) Å compared with 3.290 (1) Å in the first instance.

**Compound 9.** The crystal was photographed on Weissenberg and precession cameras to establish the space group and cell. The density was measured by flotation in $CCl_4/CHBr_3$ ($\rho_{measd} = 1.869$ g cm$^{-3}$) and revealed the presence of $CH_2Cl_2$ solvent in the crystal structure. Zr-filtered Mo radiation and a Picker 4-circle diffractometer automated by a PDP-11/10 computer were used. The unit cell was refined by least squares from 13 pairs of +2θ measurements. Crystal data comparable to those for **1a** and **1b** are given in Table I. Intensities were measured by a stepped scan of 200 steps of 0.01° in 2θ counting for 0.25 s/step and a background count of 25 s at each end of the scan. Measurements were done in the range 2θ = 0–40° (*h* unrestricted, *k*, *l* ≥ 0. Three standards 0,14,0, 400, and 006 preceded each batch of 50 reflections and were used in scaling; there were instrumental fluctuations affecting all standards alike, but no noticeable decline in intensity. Absorption corrections were done by numerical integration using a 14 × 6 × 14 Gaussian grid, and the transmission range was 0.23–0.40. After Lorentz and polarization corrections, the structure was solved by the Patterson function and refined by using SHELX. The atomic scattering factors were as described above. The weights used were $w = 1/(\sigma^2(F) + 0.0001F^2)$. The refinement converged at *R* = 0.050 and $R_w = (\sum w\Delta^2/\sum wF_o^2)^{1/2} = 0.0616$ for $F_o > 4\sigma(F)$, with 3003 reflections used to determine 559 parameters. The final difference map used to check the structure had a maximum of 0.99 e Å$^{-3}$ and indicated no serious errors or omissions. The fractional coordinates for **9** are given in Table IV.

## Results and Discussion

With the characterization[8] by X-ray diffraction of the scarlet, crystalline product obtained from the reaction between *trans*-$Ir(PPh_3)_2(CO)Cl$ and the pyrazolide anion as the pyrazolyl-bridged dimer (**1**), a systematic route to this complex was sought and was established in the manner set out in Scheme I. Thus, the familiar[21] dimer $[Ir(COD)Cl]_2$ may be converted easily and in high yield, by treatment with pyrazole (pzH) and $NEt_3$ in THF, to the purple-red, crystalline pyrazolyl-bridged complex $[Ir(COD)(\mu\text{-pz})]_2$ (**2**), the rhodium analogue of which has been reported previously.[11] Bubbling

---

(17) Germain, G.; Main, P.; Woolfson, M. M. *Acta Crystallogr., Sect. A: Cryst. Phys., Diffr., Theor. Gen. Crystallogr.* **1971**, *A27*, 368.

(18) Sheldrick, G. M. "SHELX, A System of Computer Programs for X-ray Structure Determination"; University of Cambridge: Cambridge, England, 1976.

(19) Cromer, D. T.; Mann, B. *Acta Crystallogr., Sect. A: Cryst. Phys., Diffr., Theor. Gen. Crystallogr.* **1968**, *A24*, 321.

(20) Cromer, D. T.; Liberman, D. *J. Chem. Phys.* **1970**, *53*, 1891.

(21) Herde, J. L.; Lambert, J. C.; Senoff, C. V. *Inorg. Synth.* **1974**, *15*, 18.

**Table II.** Fractional Atomic Coordinates for Complex 1a

| atom | *x/a* | *y/b* | *z/c* |
|---|---|---|---|
| Ir(1) | 0.3958 (2) | 0.8454 (1) | 0.32150 (8) |
| Ir(2) | 0.3020 (2) | 0.8620 (1) | 0.17342 (8) |
| P(1) | 0.245 (1) | 0.7025 (8) | 0.3875 (5) |
| P(2) | 0.388 (1) | 0.7326 (8) | 0.1067 (5) |
| O(1) | 0.622 (5) | 0.710 (3) | 0.335 (2) |
| O(2) | 0.021 (4) | 0.693 (2) | 0.142 (2) |
| N(1) | 0.260 (4) | 0.960 (2) | 0.305 (2) |
| N(2) | 0.223 (4) | 0.967 (2) | 0.241 (2) |
| N(3) | 0.531 (4) | 0.983 (2) | 0.263 (2) |
| N(4) | 0.494 (3) | 0.996 (2) | 0.198 (1) |
| C(1) | 0.525 (7) | 0.765 (5) | 0.340 (3) |
| C(2) | 0.126 (6) | 0.758 (4) | 0.151 (3) |
| C(3) | 0.182 (5) | 1.032 (4) | 0.346 (2) |
| C(4) | 0.101 (5) | 1.086 (3) | 0.305 (2) |
| C(5) | 0.126 (5) | 1.046 (3) | 0.241 (2) |
| C(6) | 0.661 (5) | 1.078 (3) | 0.270 (2) |
| C(7) | 0.696 (4) | 1.139 (3) | 0.212 (2) |
| C(8) | 0.602 (5) | 1.087 (3) | 0.163 (2) |
| C(9) | 0.302 (4) | 0.565 (3) | 0.425 (2) |
| C(10) | 0.353 (4) | 0.487 (3) | 0.385 (2) |
| C(11) | 0.392 (5) | 0.368 (3) | 0.405 (2) |
| C(12) | 0.363 (5) | 0.339 (4) | 0.473 (2) |
| C(13) | 0.313 (5) | 0.410 (3) | 0.516 (2) |
| C(14) | 0.279 (5) | 0.532 (3) | 0.491 (2) |
| C(15) | 0.207 (5) | 0.788 (3) | 0.453 (2) |
| C(16) | 0.310 (5) | 0.882 (3) | 0.490 (2) |
| C(17) | 0.281 (5) | 0.950 (3) | 0.543 (2) |
| C(18) | 0.143 (5) | 0.948 (3) | 0.566 (2) |
| C(19) | 0.033 (6) | 0.850 (4) | 0.534 (3) |
| C(20) | 0.065 (5) | 0.781 (4) | 0.482 (2) |
| C(21) | 0.079 (4) | 0.615 (3) | 0.351 (2) |
| C(22) | 0.011 (5) | 0.675 (4) | 0.308 (2) |
| C(23) | −0.119 (5) | 0.612 (4) | 0.282 (2) |
| C(24) | −0.181 (5) | 0.481 (4) | 0.298 (2) |
| C(25) | −0.118 (6) | 0.416 (4) | 0.339 (3) |
| C(26) | 0.021 (5) | 0.485 (4) | 0.366 (2) |
| C(27) | 0.396 (5) | 0.576 (3) | 0.144 (2) |
| C(28) | 0.291 (5) | 0.516 (3) | 0.188 (2) |
| C(29) | 0.294 (5) | 0.390 (4) | 0.217 (2) |
| C(30) | 0.405 (6) | 0.334 (4) | 0.203 (3) |
| C(31) | 0.501 (5) | 0.384 (4) | 0.157 (2) |
| C(32) | 0.500 (5) | 0.515 (3) | 0.129 (2) |
| C(33) | 0.565 (6) | 0.795 (4) | 0.072 (2) |
| C(34) | 0.594 (8) | 0.805 (5) | 0.006 (3) |
| C(35) | 0.722 (9) | 0.838 (6) | −0.013 (4) |
| C(36) | 0.831 (9) | 0.873 (5) | 0.032 (4) |
| C(37) | 0.813 (7) | 0.865 (4) | 0.096 (3) |
| C(38) | 0.673 (6) | 0.826 (4) | 0.124 (2) |
| C(39) | 0.288 (4) | 0.679 (3) | 0.032 (2) |
| C(40) | 0.258 (4) | 0.552 (3) | 0.007 (2) |
| C(41) | 0.172 (5) | 0.514 (3) | −0.047 (2) |
| C(42) | 0.122 (5) | 0.606 (4) | −0.080 (2) |
| C(43) | 0.142 (5) | 0.738 (4) | −0.055 (2) |
| C(44) | 0.233 (5) | 0.771 (3) | 0.002 (2) |

**Scheme I**

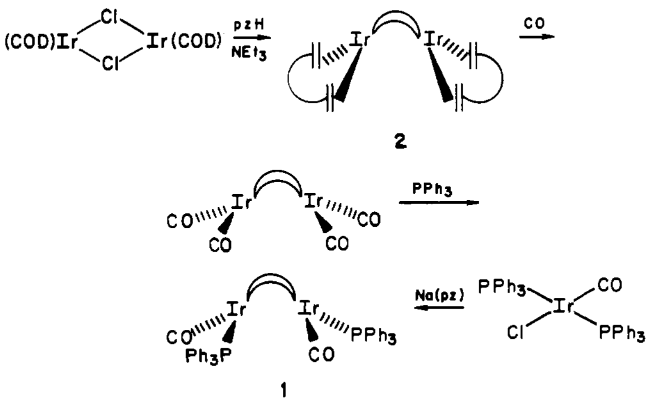

**Table III.** Fractional Atomic Coordinates for Complex 1b

| atom | *x/a* | *y/b* | *z/c* |
|---|---|---|---|
| Ir(1) | 0.35423 (6) | 0.5885 (1) | 0.32661 (3) |
| Ir(2) | 0.21147 (7) | 0.7265 (1) | 0.38818 (3) |
| P(1) | 0.4511 (4) | 0.4380 (7) | 0.3580 (2) |
| P(2) | 0.0852 (5) | 0.6136 (7) | 0.3812 (2) |
| O(1) | 0.284 (1) | 0.392 (2) | 0.2598 (7) |
| O(2) | 0.222 (1) | 0.674 (2) | 0.4837 (8) |
| N(1) | 0.269 (1) | 0.732 (2) | 0.2960 (6) |
| N(2) | 0.208 (1) | 0.790 (2) | 0.3234 (6) |
| N(3) | 0.396 (1) | 0.748 (2) | 0.3682 (6) |
| N(4) | 0.334 (1) | 0.812 (2) | 0.3927 (6) |
| C(1) | 0.313 (2) | 0.463 (3) | 0.2888 (9) |
| C(2) | 0.216 (2) | 0.695 (3) | 0.442 (1) |
| C(3) | 0.256 (2) | 0.783 (3) | 0.2554 (8) |
| C(4) | 0.187 (2) | 0.871 (3) | 0.2545 (8) |
| C(5) | 0.156 (2) | 0.874 (3) | 0.2954 (8) |
| C(6) | 0.476 (1) | 0.807 (2) | 0.3830 (8) |
| C(7) | 0.463 (2) | 0.900 (3) | 0.4138 (8) |
| C(8) | 0.377 (2) | 0.908 (3) | 0.4202 (8) |
| C(9) | 0.452 (1) | 0.268 (2) | 0.3304 (7) |
| C(10) | 0.528 (2) | 0.217 (3) | 0.3136 (8) |
| C(11) | 0.530 (2) | 0.089 (4) | 0.296 (1) |
| C(12) | 0.452 (2) | 0.008 (3) | 0.292 (1) |
| C(13) | 0.378 (2) | 0.057 (3) | 0.3134 (8) |
| C(14) | 0.379 (1) | 0.192 (3) | 0.3290 (8) |
| C(15) | 0.563 (1) | 0.494 (2) | 0.3586 (8) |
| C(16) | 0.587 (2) | 0.563 (3) | 0.320 (1) |
| C(17) | 0.674 (2) | 0.614 (4) | 0.318 (1) |
| C(18) | 0.730 (2) | 0.583 (4) | 0.353 (1) |
| C(19) | 0.710 (2) | 0.516 (4) | 0.390 (1) |
| C(20) | 0.623 (2) | 0.475 (3) | 0.3937 (9) |
| C(21) | 0.437 (1) | 0.393 (2) | 0.4142 (7) |
| C(22) | 0.397 (1) | 0.482 (3) | 0.4432 (8) |
| C(23) | 0.385 (2) | 0.448 (3) | 0.4851 (9) |
| C(24) | 0.413 (2) | 0.324 (3) | 0.505 (1) |
| C(25) | 0.459 (2) | 0.229 (3) | 0.476 (1) |
| C(26) | 0.468 (2) | 0.266 (3) | 0.4326 (9) |
| C(27) | 0.017 (2) | 0.644 (3) | 0.3281 (9) |
| C(28) | 0.047 (2) | 0.589 (3) | 0.2925 (9) |
| C(29) | 0.003 (2) | 0.618 (3) | 0.250 (1) |
| C(30) | −0.066 (2) | 0.699 (3) | 0.249 (1) |
| C(31) | −0.093 (2) | 0.763 (3) | 0.287 (1) |
| C(32) | −0.049 (2) | 0.735 (3) | 0.3296 (9) |
| C(33) | 0.100 (2) | 0.421 (3) | 0.3832 (8) |
| C(34) | 0.177 (2) | 0.367 (3) | 0.3958 (9) |
| C(35) | 0.190 (2) | 0.221 (3) | 0.400 (1) |
| C(36) | 0.123 (2) | 0.143 (3) | 0.387 (1) |
| C(37) | 0.046 (2) | 0.184 (4) | 0.370 (1) |
| C(38) | 0.028 (2) | 0.332 (3) | 0.370 (1) |
| C(39) | 0.013 (2) | 0.650 (3) | 0.4237 (8) |
| C(40) | −0.046 (2) | 0.554 (3) | 0.4378 (9) |
| C(41) | −0.098 (2) | 0.592 (4) | 0.473 (1) |
| C(42) | −0.101 (2) | 0.718 (4) | 0.487 (1) |
| C(43) | −0.043 (3) | 0.814 (5) | 0.479 (1) |
| C(44) | 0.011 (2) | 0.783 (4) | 0.440 (1) |
| C(45) | 0.316 | 0.514 | 0.098 |
| C(46) | 0.286 | 0.559 | 0.054 |
| C(47) | 0.193 | 0.609 | 0.074 |
| C(48) | 0.203 | 0.653 | 0.122 |
| C(49) | 0.220 | 0.525 | 0.146 |
| C(50) | 0.243 | 0.457 | 0.100 |

CO through a solution in THF of compound **2** leads to a rapid color change to yellow. Repetition using a suspension of **2** in hexane also affords a yellow solution, which shows IR bands at 2083, 2070, and 2011 cm$^{-1}$, consistent with the presence of the tetracarbonyldiiridium complex $[Ir(CO)_2(\mu\text{-pz})]_2$, although the latter appears to be stable only in the presence of excess CO and attempts to isolate it met with failure. Subsequent addition of $PPh_3$ (2 mol equiv) to these yellow solutions generated compound (**1**), >85% overall yield. No reaction occurred, however, between complex **2** and $PPh_3$ (4.5 mol equiv) in refluxing hexane (4 h); neither was there any change during treatment of complex **1** under similar conditions with a further 2 mol equiv of $PPh_3$. By contrast we have since observed direct displacement of COD from compound **2** by the chelating phosphines diphos or dppm or by $PF_3$.[22] Re-

---

[22] Fjeldsted, D. O. K.; Stobart, S. R., unpublished results.

Table IV. Fractional Atomic Coordinates for Complex 9[a]

| atom | *x/a* | *y/b* | *z/c* |
|---|---|---|---|
| Ir(1) | 0.45173 (4) | 0.21400 (3) | 0.43283 (7) |
| Ir(2) | 0.52351 (4) | 0.28581 (3) | 0.57029 (7) |
| Cl(1) | 0.4478 (4) | 0.1586 (2) | 0.2652 (5) |
| Cl(2) | 0.6381 (3) | 0.3416 (2) | 0.6244 (5) |
| Cl(3) | 0.8197 (4) | 0.1730 (3) | 0.4747 (7) |
| Cl(4) | 0.6114 (4) | 0.3275 (3) | 0.0778 (6) |
| Cl(5) | 0.2468 (9) | 0.0595 (5) | −0.106 (2) |
| Cl(6) | 0.2023 (9) | 0.0059 (5) | 0.1012 (13) |
| Cl(7) | −0.0088 (11) | 0.4976 (7) | 0.7011 (13) |
| Cl(8) | 0.1432 (11) | 0.4482 (8) | 0.694 (2) |
| P(1) | 0.4266 (3) | 0.1528 (2) | 0.5610 (5) |
| P(2) | 0.4266 (3) | 0.3465 (2) | 0.5661 (5) |
| O(1) | 0.2688 (10) | 0.2425 (6) | 0.386 (2) |
| O(2) | 0.5000 (9) | 0.2572 (6) | 0.8209 (13) |
| N(1) | 0.5788 (10) | 0.2030 (6) | 0.4684 (14) |
| N(2) | 0.6137 (9) | 0.2343 (6) | 0.546 (2) |
| N(3) | 0.4928 (10) | 0.2650 (6) | 0.323 (2) |
| N(4) | 0.5389 (10) | 0.2990 (6) | 0.387 (2) |
| C(1) | 0.339 (2) | 0.2310 (8) | 0.410 (2) |
| C(2) | 0.506 (2) | 0.2684 (8) | 0.723 (2) |
| C(3) | 0.6413 (13) | 0.1761 (9) | 0.425 (2) |
| C(4) | 0.7178 (13) | 0.1945 (8) | 0.489 (2) |
| C(5) | 0.6968 (12) | 0.2298 (8) | 0.562 (2) |
| C(6) | 0.5066 (13) | 0.2701 (8) | 0.204 (2) |
| C(7) | 0.5640 (13) | 0.3068 (8) | 0.204 (2) |
| C(8) | 0.5864 (11) | 0.3242 (7) | 0.321 (2) |
| C(9) | 0.257 (3) | 0.057 (2) | 0.058 (4) |
| C(10) | 0.043 (3) | 0.4434 (13) | 0.651 (4) |
| C(11) | 0.4005 (13) | 0.1642 (9) | 0.715 (2) |
| C(12) | 0.4403 (14) | 0.1443 (8) | 0.818 (2) |
| C(13) | 0.4119 (15) | 0.1517 (10) | 0.933 (2) |
| C(14) | 0.3430 (14) | 0.1810 (9) | 0.945 (2) |
| C(15) | 0.3028 (13) | 0.2003 (8) | 0.839 (2) |
| C(16) | 0.3304 (13) | 0.1928 (8) | 0.730 (2) |
| C(21) | 0.3376 (11) | 0.1137 (8) | 0.514 (2) |
| C(22) | 0.2849 (13) | 0.1189 (7) | 0.405 (2) |
| C(23) | 0.2162 (14) | 0.0896 (9) | 0.376 (2) |
| C(24) | 0.2067 (14) | 0.0507 (10) | 0.457 (3) |
| C(25) | 0.259 (2) | 0.0435 (10) | 0.561 (3) |
| C(26) | 0.3248 (13) | 0.0740 (8) | 0.590 (2) |
| C(31) | 0.5187 (13) | 0.1161 (8) | 0.581 (2) |
| C(32) | 0.5163 (14) | 0.0750 (9) | 0.511 (2) |
| C(33) | 0.592 (2) | 0.0458 (9) | 0.522 (3) |
| C(34) | 0.663 (2) | 0.0599 (10) | 0.597 (3) |
| C(35) | 0.6614 (15) | 0.1017 (10) | 0.667 (2) |
| C(36) | 0.5899 (12) | 0.1289 (8) | 0.659 (2) |
| C(41) | 0.3109 (12) | 0.3323 (7) | 0.554 (2) |
| C(42) | 0.2868 (12) | 0.3026 (7) | 0.642 (2) |
| C(43) | 0.1986 (14) | 0.2943 (8) | 0.643 (2) |
| C(44) | 0.1410 (13) | 0.3160 (10) | 0.566 (2) |
| C(45) | 0.166 (2) | 0.3498 (10) | 0.482 (3) |
| C(46) | 0.2539 (13) | 0.3572 (10) | 0.477 (2) |
| C(51) | 0.4331 (13) | 0.3864 (7) | 0.698 (2) |
| C(52) | 0.375 (2) | 0.4233 (9) | 0.690 (2) |
| C(53) | 0.378 (2) | 0.4541 (9) | 0.785 (3) |
| C(54) | 0.429 (2) | 0.4470 (11) | 0.895 (3) |
| C(55) | 0.4862 (14) | 0.4111 (9) | 0.899 (2) |
| C(56) | 0.4877 (12) | 0.3791 (7) | 0.803 (2) |
| C(61) | 0.4424 (12) | 0.3872 (8) | 0.441 (2) |
| C(62) | 0.4922 (14) | 0.4261 (7) | 0.465 (2) |
| C(63) | 0.510 (2) | 0.4558 (9) | 0.366 (2) |
| C(64) | 0.472 (2) | 0.4457 (9) | 0.253 (2) |
| C(65) | 0.421 (2) | 0.4019 (9) | 0.227 (2) |
| C(66) | 0.4069 (12) | 0.3735 (8) | 0.322 (2) |

[a] Estimated standard deviations are given in parentheses.

action of substituted pyrazoles according to Scheme I has afforded a family of COD dimers related to compound **2**, several of which will react with $PPh_3$ to provide analogues[23] of complex **1**; alternately other tertiary phosphines may be introduced to generate further analogues of **1**.

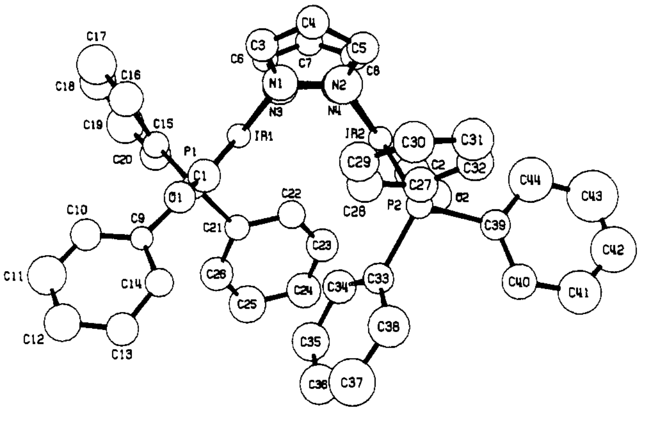

**Figure 1.** ORTEP plot of the molecular structure of compound **1a**.

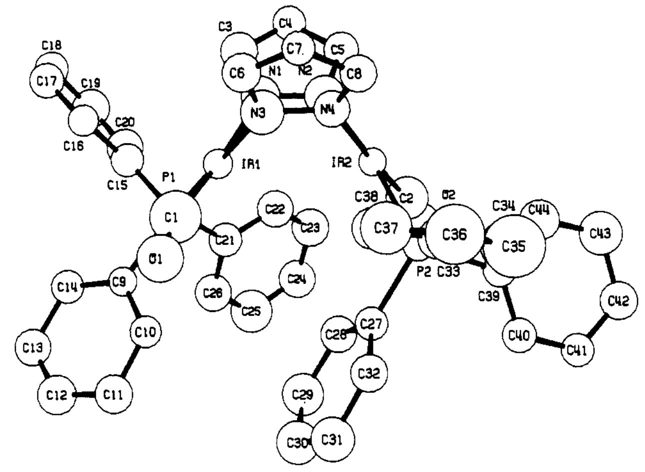

**Figure 2.** ORTEP plot of the molecular structure of compound **1b**.

The IR spectrum of complex **1** (KBr pellet) showed a single strong $\nu_{CO}$ absorption at 1965 cm$^{-1}$, while the $^1H$ NMR spectrum (THF-$d_8$, 90 MHz) included peaks at $\delta$ 5.77 (t) and 6.50 (d) in 1:1 ratio, assigned respectively to the 4-H and to one of the inequivalent 3-H or 5-H of the pyrazolyl bridge. The resonance due to the third bridge proton (5-H or 3-H) is assumed to lie under the complex $PPh_3$ envelope at $\delta$ 7.34–7.68; this is supported by the appearance of the $^1H$ spectrum for complex **2**, which in addition to a high-field COD pattern shows a triplet at $\delta$ 6.22 and a doublet at $\delta$ 7.48 ($^3J$ = 1.9 Hz; 1:2 ratio, bridge 4-H and equivalent 3-H and 5-H, respectively). Comparison of these data also indicates that the bridge 3-H, 4-H, and 5-H magnetic environments are sensitive to the character of the terminal ligands at Ir. The $^{31}P$ NMR spectrum ($CH_2Cl_2$, 24.3 MHz) of compound **1** consisted of a sharp singlet at −122.4 ppm and showed no changes down to −85 °C.

The spectral data may be interpreted in terms of existence of **1** as a single isomer in solution; the presence of only one 4-H proton environment suggests the trans configuration (A), rather than (B) which contains nonequivalent 4-H sites. The former arrangement is also that found[8] in the solid state, as

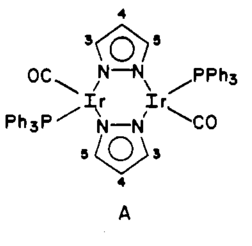

A

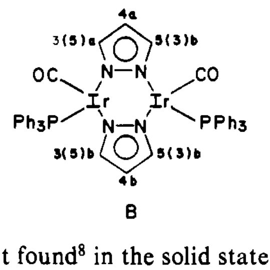

B

---

[23] With certain pyrazoles having sterically demanding 3,5-substituents, mononuclear pyrazolyl–iridium(I) complexes are isolable. The relationship between these species and the binuclear (dimeric) systems will be discussed in a forthcoming paper.

**Table V.** Important Bond Distances (Å) and Angles (deg) for **1a**, **1b**, and **9**

| | 1a | 1b | 9 |
|---|---|---|---|
| | Bond Lengths | | |
| Ir(1)–Ir(2) | 3.163 (2) | 3.290 (1) | 2.737 (1) |
| Ir–Cl(1) | | | 2.440 (6) |
| Ir–Cl(2) | | | 2.446 (6) |
| Ir(1)–P(1) | 2.26 (1) | 2.262 (6) | 2.316 (6) |
| Ir(2)–P(2) | 2.24 (1) | 2.244 (7) | 2.316 (6) |
| Ir(1)–N(1) | 2.06 (3) | 2.10 (2) | 2.04 (2) |
| Ir(2)–N(2) | 2.02 (4) | 2.07 (2) | 2.09 (2) |
| Ir(2)–N(3) | 2.07 (4) | 2.08 (2) | 2.05 (2) |
| Ir(2)–N(4) | 2.10 (2) | 2.07 (2) | 2.10 (2) |
| Ir(1)–C(1) | 1.76 (6) | 1.77 (3) | 1.84 (3) |
| Ir(2)–C(2) | 1.89 (5) | 1.67 (3) | 1.81 (2) |
| C(1)–O(1) | 1.20 (7) | 1.18 (3) | 1.17 (3) |
| C(2)–O(2) | 1.08 (5) | 1.29 (3) | 1.15 (3) |
| N(1)–N(2) | 1.36 (4) | 1.42 (2) | 1.33 (2) |
| N(3)–N(4) | 1.36 (3) | 1.41 (2) | 1.37 (2) |
| P–C (av) | 1.81 | 1.84 | 1.85 |
| | Bond Angles | | |
| P(1)–Ir(1)–N(1) | 93 (1) | 177.4 (5) | 89.5 (5) |
| P(1)–Ir(1)–N(3) | 178 (1) | 93.0 (5) | 171.3 (5) |
| P(1)–Ir(1)–C(1) | 91 (2) | 91.7 (8) | 93.5 (7) |
| N(1)–Ir(1)–N(3) | 85 (1) | 86.5 (7) | 81.8 (6) |
| C(1)–Ir(1)–N(1) | 174 (2) | 89 (1) | 172.9 (8) |
| C(1)–Ir(1)–N(3) | 90 (2) | 175 (1) | 95.2 (8) |
| P(2)–Ir(2)–N(2) | 174.8 (8) | 95.3 (6) | 171.0 (5) |
| P(2)–Ir(2)–N(4) | 97 (1) | 174.2 (6) | 89.3 (5) |
| P(2)–Ir(2)–C(2) | 89 (2) | 89 (1) | 93.5 (8) |
| N(2)–Ir(2)–N(4) | 84 (1) | 84.5 (7) | 81.7 (6) |
| N(2)–Ir(2)–C(2) | 91 (2) | 173 (1) | 95.5 (9) |
| N(4)–Ir(2)–C(2) | 175 (2) | 92 (1) | 173.9 (9) |
| Ir(1)–C(1)–O(1) | 168 (7) | 172 (2) | 175 (2) |
| Ir(2)–C(2)–O(2) | 178 (5) | 178 (3) | 176 (2) |
| Ir(1)–N(1)–N(2) | 114 (3) | 115 (1) | 111.0 (12) |
| Ir(1)–N(3)–N(4) | 117 (2) | 117 (1) | 112.4 (12) |
| Ir(2)–N(2)–N(1) | 118 (2) | 118 (1) | 108.4 (11) |
| Ir(2)–N(4)–N(3) | 114 (2) | 116 (1) | 105.5 (12) |

| | bond angles for 9 | | bond angles for 9 |
|---|---|---|---|
| N(1)–Ir(1)–Ir(2) | 70.2 (5) | N(3)–Ir(1)–Ir(2) | 69.9 (5) |
| N(2)–Ir(2)–Ir(1) | 69.5 (4) | N(4)–Ir(2)–Ir(1) | 71.3 (5) |
| C(1)–Ir(1)–Ir(2) | 102.8 (7) | C(2)–Ir(2)–Ir(1) | 102.6 (8) |
| P(1)–Ir(1)–Ir(2) | 108.3 (1) | P(2)–Ir(2)–Ir(1) | 108.3 (1) |
| Cl(1)–Ir(1)–Ir(2) | 152.8 (1) | Cl(2)–Ir(2)–Ir(1) | 152.0 (1) |
| N(1)–Ir(1)–Cl(1) | 89.7 (5) | N(2)–Ir(2)–Cl(2) | 89.5 (5) |
| N(3)–Ir(1)–Cl(1) | 89.7 (5) | N(4)–Ir(2)–Cl(2) | 87.9 (5) |
| C(1)–Ir(1)–Cl(1) | 96.7 (7) | C(2)–Ir(2)–Cl(2) | 97.5 (8) |
| P(1)–Ir(1)–Cl(1) | 89.0 (2) | P(2)–Ir(2)–Cl(2) | 89.4 (2) |

illustrated in Figures 1 and 2 for the unsolvated form (**1a**) and the hexane solvate (**1b**), respectively. Important bond distances and angles are listed in Table V. The cyclic bridged framework deviates substantially from planarity, adopting a boat conformation, which in conjunction with the trans disposition of the terminal ligands across the $Ir_2$ vector results in a dissymmetric (enantiomeric) structure possessing $C_2$ molecular symmetry. This effect also brings the two Ir centers into close proximity: from Table VI it can be seen that the intermetallic separation of 3.163 Å in **1a** is extremely short when compared with those found in related pyrazolyl-bridged dimes, including those of first-row transition elements. Shorter distances have been observed only in compounds like **9** (see below), characterization of which has established that oxidation of complex **1** may be accompanied by formation of a metal–metal bond without disruption of the bridging pyrazolyl framework.

**Table VI.** Intermetallic Separations in Bis(pyrazolyl)-Bridged Complexes for Which a Boat Conformation Has Been Established for the Bridging Framework

| compd | M–M, Å |
|---|---|
| $(Et_3P)_2Pt(\mu\text{-}pz)_2Cr(CO)_4$[a] | 3.686 (3) |
| $[Rh(\mu\text{-}pz)(CO)(P(OPh)_3)]_2$[b] | 3.568 |
| $[Co(NO)_2(\mu\text{-}dpz)]_2$[c] | 3.417 (4) |
| $[Et_4N][Ni_2(NO)_2(\mu\text{-}dpz)_3]$[c] | 3.439 (1) |
| $[Et_4N][Ni_2(NO)_2(\mu\text{-}dpz)_2I]$[c] | 3.307 (1) |
| $[Pd(\pi\text{-}C_3H_5)(\mu\text{-}dpz)]_2$[d] | 3.343 |
| $[Fe(NO)_2(\mu\text{-}dpz)]_2$[c] | 3.3359 (3) |
| **1b**[e] | 3.290 (1) |
| $[Rh(\mu\text{-}dpz)(CS)(PPh_3)]_2$[f] | 3.220 |
| $[Ir(COD)(\mu\text{-}pz)]_2$[g] | 3.216 (1) |
| $Rh_2(\mu\text{-}dpz)_2(PPh_3)_2I_2(\mu\text{-}CO)$[h] | 3.20 |
| **1a**[e] | 3.163 (1) |

[a] Stobart, S. R.; Dixon, K. R.; Eadie, D. T.; Atwood, J. L.; Zaworotko, M. J. *Angew. Chem., Int. Ed. Engl.* 1980, *19*, 931. [b] Reference 10. [c] Chong, K. S.; Rettig, S. J.; Storr, A.; Trotter, J. *Can. J. Chem.* 1979, *57*, 3099, 3119. [d] Henslee, G. W.; Oliver, J. D. *J. Cryst. Mol. Struct.* 1977, *7*, 137. [e] This work. [f] Uson, R.; Oro, L. A.; Ciriano, M. A.; Carmona, D.; Tiripicchio, A.; Tiripicchio Camellini, M. *J. Organomet. Chem.* 1982, *224*, 69. [g] Reference 1. [h] Reference 14.

Close approach of formally nonbonded metal centers has previously been noted, for example in a number of chloro-bridged dirhodium complexes for which the structural data have been discussed[24] in terms of weak intra- (and in at least one case[24a] also inter-) molecular metal–metal interactions. An elegant experimental demonstration of such an effect in the cation $Rh_2[(\mu\text{-}CN)(CH_2)_3CN]_4^{2+}$ has recently been provided by Gray et al.:[25] from both polarized single-crystal and resonance Raman spectra it was shown that the Rh–Rh interaction is stronger in the first excited state than in the ground state, with a nonzero Rh–Rh bond order in the latter arising from configurational mixing of filled $\sigma,\sigma^*$ orbitals ($2a_{1g}$ and $2a_{2u}$ for $D_{4h}$ symmetry) derived principally from metal $4d_{z^2}$ atomic orbitals with unoccupied levels of the same symmetry ($2a_{1g}$ and $2a_{2u}$ combinations of metal $5p_z$ orbitals). Similar considerations may be pertinent to a description of the orbital overlap made possible by the short $Ir_2$ separations in complex **1** and its COD analogue **2** but are apparently contradicted by crystallographic evidence for unusual sensitivity of the intermetallic distance in compound **1** to crystal packing forces. Thus, in the hexane solvate **1b** the $Ir_2$ separation at 3.290 Å is longer by 0.13 Å than in **1a** (unsolvated), although in neither structure is there any close (<4 Å) intermolecular approach to Ir and in all other respects the two are identical within experimental error (Table V). A somewhat larger change (0.16 Å) in the opposite sense observed[26] for $[Rh(Cl)(CO)(\mu\text{-}Me_2AsCH_2AsMe_2)]_2$, in which the $Rh_2$ separation of 3.396 Å contracts to 3.236 Å in the $CH_2Cl_2$ solvate, has been projected as evidence against any direct metal–metal interaction in this dimeric system. Metal–ligand distances and angles in compound **1a**,**b** are normal (Table V), and deviation from planarity in coordination around each Ir atom is less than 0.10 Å. The trans arrangement excludes steric interference between the $PPh_3$ ligands, and planarity of the phenyl- and pyrazolyl-ring systems is also maintained to within 0.05 Å. By comparison, in the phosphite complex $[Rh(P(OPh)_3)(CO)(\mu\text{-}pz)]_2$ the $M_2$ distance is much longer (3.57 Å), but a trans conformation is adopted;[10] conversely, the thiolato-bridged dimer (**5**, R = OMe) is cis in the crystalline state.[12]

---

(24) (a) Dahl, L. F.; Martell, C.; Wampler, D. J. *J. Am. Chem. Soc.* **1961**, *83*, 1761. (b) Oberhansli, W. E.; Dahl, L. F. *J. Organomet. Chem.* **1965**, *3*, 43. (c) Coetzer, J.; Gafner, G. *Acta Crystallogr., Sect. B: Struct. Crystalogr. Cryst. Chem.* **1970**, *26*, 985. (d) Drew, M. G. B.; Nelson, S. M.; Sloan, M. *J. Chem. Soc., Dalton Trans.* **1973**, 1484. (e) Bonnet, J. J.; Kalck, P.; Maisonnet, A.; Poilblanc, R. *Inorg. Chem.* **1975**, *14*, 743.

(25) Rice, S. F.; Gray, H. B. *J. Am. Chem. Soc.* **1981**, *103*, 1593. Dallinger, R. F.; Miskowski, V. M.; Gray, H. B.; Woodruff, W. H. *Ibid.* **1981**, *103*, 1595.

(26) Cowie, M.; Dwight, S. K. *Inorg. Chem.* **1981**, *20*, 1534.

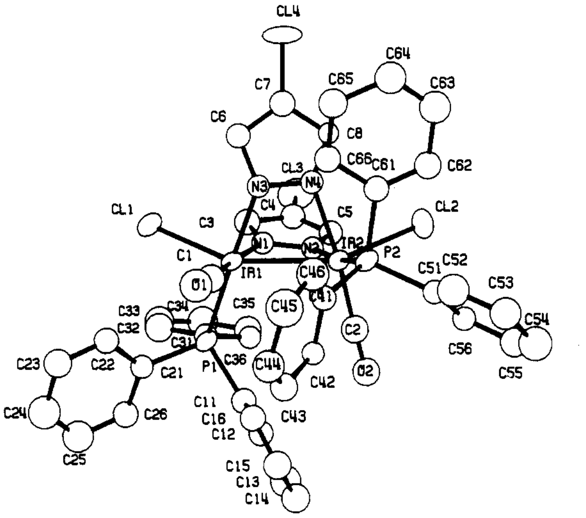

**Figure 3.** ORTEP plot of the molecular structure of compound **9**.

Addition to a solution of compound **1** of 1 equiv of $I_2$ or $Br_2$ rapidly precipitated bright yellow adducts **7** and **8**. These products proved to be insufficiently soluble in common organic solvents to allow satisfactory NMR measurements and attempts at crystallization were unsuccessful, but microanalytical data were appropriate for the 1:1 formulation (C); support for this was also provided by observation of an IR absorption near 1385 $cm^{-1}$ that seems to be diagnostic for the bridging pyrazolyl fragment. Each adduct showed two $\nu_{CO}$ bands in the IR spectrum, shifted to higher wavenumber than that in **1** (**7**, 2021, 2012 $cm^{-1}$; **8**, 2020, 2010 $cm^{-1}$), but rather lower in energy than the established range for carbonyl derivatives of Ir(III), consistent with the proposed dissymmetric dimeric structures in which each metal center may be assigned a formal II oxidation state. Treatment of complex **1** in THF solution with $Cl_2$ gas led to immediate formation of an analogue (**9**), which was considerably more soluble than **7** or **8** and for which crystals suitable for X-ray diffractometry were obtained from $CH_2Cl_2$ solution. This product showed $\nu_{CO}$ at 2030 and 2019 $cm^{-1}$ and a single $^{31}P$ NMR resonance at −146.5 ppm, while in the $^1H$ NMR spectrum a singlet resonance at $\delta$ 8.20 replaced the multiplet signals assigned to bridge protons for **1**; this loss of proton–proton coupling together with the shift to low field are indicative of Cl substitution at the 4-position in the pyrazolyl ring.

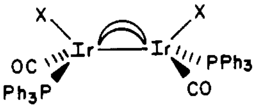

C: X=I, Br

The molecular geometry of complex **9** is shown in Figure 3. Bond distances and angles are included in Table V. The trans arrangement adopted by compound **1** is retained, but in addition to occupation of the apical position at each Ir center by a chlorine atom, the $Ir_2$ separation has contracted dramatically, to 2.737 Å. This is ca. twice the estimated covalent radius[27] for Ir, falling at the upper end of the range of distances attributed to Ir–Ir single bonds (Table VII). The structural modifications therefore correspond exactly to those earlier proposals[4] expressed in terms of eq 1 and clearly identify **9** as the product of a formal two-fragment, two-center oxidative addition. Substitution by Cl into the pyrazolyl group as suggested by the NMR results is also confirmed (Figure 3; Table V); attack has occurred at the 4-position as expected for an electrophilic reaction, stressing simultaneously the aromatic character of the heterocyclic ring system and resistance to displacement from its bridging function. Each of the two Ir–Cl bonds inclines at 152° to the Ir–Ir bond, lying almost exactly perpendicular (Table V) to the equatorial coordination environment around the metal. The Ir–Cl bond is elongated (mean 2.443 Å) compared with reported values for a variety of Ir(I) or Ir(III) species, e.g.[28] chlorocarbonyl(2-(diphenylphosphino)-*N*,*N*-dimethylethylamine)iridium(I), $(PMe_2Ph)_3IrCl_3$, or $Ir_2Cl_6(Et_2S)_4$, although a very long Ir–Cl (2.549 Å) has been observed trans to H in[29] (1-phenylallyl)chlorohydridobis(triphenylphosphine)iridium(III). Decrease in electron density at the metal accompanying oxidation from Ir(I) to (formally) Ir(II) may account for the lengthening of Ir–P from 2.25 Å (mean) in complex **1** to 2.316 Å in **9**.

Table VII. Ir–Ir Single-Bond Distances (Å)

| | |
|---|---|
| 9 | 2.737 |
| $Ir_2(\eta\text{-}C_5H_5)_2(CO)_2(\mu\text{-}C_6H_4)^a$ | 2.718 |
| $[Ir(PPh_3)(NO)_2]_2{}^b$ | 2.717 |
| $[Ir(PMe_2Ph)(CO)(\mu\text{-}t\text{-}BuS)(I)]_2{}^c$ | 2.703 |
| $[Ir[P(OPh)_3](CO)(\mu\text{-}dpz)(I)]_2{}^d$ | 2.688 |
| $Ir_4(CO)_{12}{}^e$ | 2.68 |
| $Ir_2(PPh_3)_2(CO)_2(Br)_2(\mu\text{-}C_{10}H_4S_4)^f$ | 2.676 |
| $[Ir[P(OMe)_3](CO)(\mu\text{-}t\text{-}BuS)(H)]_2{}^g$ | 2.673 |

[a] Single *o*-phenylene bridge: Rausch, M. D.; Gastinger, R. G.; Gardner, S. A.; Brown, R. K.; Wood, J. S. *J. Am. Chem. Soc.* 1977, *99*, 7870. [b] Unsupported Ir–Ir bond: Angoletta, M.; Gianfranco, C.; Manassero, M.; Sansoni, M. *J. Chem. Soc., Chem. Commun.* 1973, 789. [c] Reference 13. [d] Reference 14. [e] Churchill, M. R.; Hutchinson, J. P. *Inorg. Chem.* 1978, *17*, 3528–3535. The structure of $Ir_4(CO)_{12}$ was first determined by G. R. Wilkes in the laboratories of Professor L. F. Dahl: Wilkes, G. R. Ph.D. Thesis, University of Wisconsin, Madison, 1965. [f] Bridging tetrathionaphthalene unit: Teo, B.-K.; Snyder-Robinson, P. A. *J. Chem. Soc., Chem. Commun.* 1979, 255. [g] Reference 12.

Formation of an Ir–Ir bond in **9** results predictably in a substantial decrease from 73.1 (**1a**) and 76.3 (**1b**) to 51.6° in the dihedral angle between the (equatorial) IrNNPC planes; this does not, however, introduce steric repulsion between the halves of the dimer, and in fact the most significant departure from equatorial planarity at Ir is displacements of $C_{CO}$ (0.15, 0.12 Å) *toward* the opposite Ir atom. A further and most interesting structural effect emerges from an examination of the way in which the dihedral angle between the planar bridging ligands alters as the $Ir_2$ distance contracts. An arbitrary angle connecting the midpoints of N(1)–N(2), Ir(1)–Ir(2), and N(3)–N(4) closes from 99.1 (**1b**) through 96.9 (**1a**) to 88.1° in **9**. In **1a** or **1b** each metal atom is close to being coplanar with a pyrazolyl ligand, but the two bridges, which resemble the wings of a butterfly, are slightly splayed apart from one other along the N–N lines. In the chlorine adduct (**9**) the angle between the "butterfly wings" has closed by over 35°; this arises both through the reduction in the angle between the midpoints and pivoting about the N–N bonds, such that the dihedral angle between the pyrazolyl rings is 109.1° in **1b** and 101.4° in **1a** but only 64.8° in **9**. We have observed related behavior[1a] on oxidation of COD analogues like **2**, and this flexibility may be critical in allowing the exobidentate bridge to accommodate remarkably large changes in bridging span. In a five-membered N heterocycle the idealized internal angle is 108°, predisposing the molecule to coordinate bond formation displaced somewhat from the plane of the ring system. This combines with the reduction in IrNN

---

(27) Porterfield, W. W. In "Concepts of Chemistry"; W. W. Norton and Co.: New York, 1972. "Cambridge Data Base Manual"; CISTI: NRC Canada, 1981; Appendix E, p 131.

(28) Roundhill, D. M.; Bechtold, R. A.; Roundhill, S. G. N. *Inorg. Chem.* **1980**, *19*, 284. Williams, A. F.; Flack, H. D.; Vincent, M. G. *Acta Crystallogr.* **1980**, *36*, 1206. *Ibid.* **1981**, *37*, 814.

(29) Tulip, T. H.; Ibers, J. A. *J. Am. Chem. Soc.* **1978**, *100*, 3252.

*Inorg. Chem.* **1984**, *23*, 4057-4064

angle (116° in **1a**,**b**; 109.3° in **9**) accompanying Ir–Ir bond formation to force the N atoms somewhat toward tetrahedral geometry. Intramolecular contacts are significant (~3.2 Å) in one region of molecule **9**, between the chloropyrazolyl bridges and phenyl rings C(31)–C(36) and C(61)–C(66). This twists the bridging ligands with respect to the Ir–Ir bond, causing Ir(1) to deviate 0.16 and 0.61 Å from the two pyrazolyl planes with Ir(2) so displaced by 0.52 and 0.23 Å.

Reaction of complex **1** with methyl iodide (1 equiv or excess) afforded a 1:1 adduct as a yellow powder (**10**), which like **7** and **8** showed poor solubility in organic solvents. Two $\nu_{CO}$ absorptions were found in the IR spectrum at 2013 and 1993 cm$^{-1}$, and the $^{31}$P NMR spectrum consisted of two resonances having equal intensity (−140.5, −141.8 ppm) attributable to $PPh_3$ ligands attached to distinguishable metal atoms. These data indicate a structure similar to C, with Me and I in apical positions at Ir as has been established crystallographically[1a] for the MeI adduct of complex **2**. By contrast, a corresponding reaction with MeBr appeared to give several products, and a bromo analogue of **10** has not yet been isolated. These observations will be consolidated as part of a more extensive examination of the reactivity of compound **1** toward functionalized organic molecules.

There is a close stereochemical relationship between the structures of compounds **1** and **9**. Both are enantiomeric ($C_2$ molecular symmetry) and share the same (trans) orientation of terminal ligands in the equatorial plane at Ir, i.e. the oxidative addition step occurs with no net ligand reorganization at the metal center. The dimer (**1**) and related complexes are in principle resolvable, either by incorporation of a chiral phosphine or related ligand or via diastereomer formation involving successive oxidative addition/reductive elimination of an optically pure substrate. Access to such resolved complexes and their relevance to reactions involving asymmetric induction or chiral recognition is being investigated.

**Acknowledgment.** We thank the NSERC (Canada) and the NSF (U.S.) for financial support of this research; S.R.S. gratefully acknowledges receipt of a University Research Grant from Imperial Oil Ltd. and a generous loan of iridium trichloride from Johnson-Matthey Inc.

**Registry No.** **1a**, 80461-91-2; **1b**, 92283-13-1; **2**, 80462-13-1; **7**, 80462-14-2; **8**, 80462-15-3; **9**, 80461-90-1; **10**, 80471-11-0; *trans*-$IrCl(CO)(PPh_3)_2$, 15318-31-7; $[Ir(C_8H_{12})Cl]_2$, 12112-67-3; $I_2$, 7553-56-2; $Br_2$, 7726-95-6; $Cl_2$, 7782-50-5; Ir, 7439-88-5; methyl iodide, 74-88-4; methyl bromide, 74-83-9; pyrazole, 288-13-1.

**Supplementary Material Available:** Listings of thermal parameters, anisotropic and isotropic temperature factors, least-squares planes, bond lengths and bond angles, and observed and calculated structure factors for compounds **1a**, **1b**, and **9** (51 pages). Ordering information is given on any current masthead page.

---

Contribution from the Laboratoire de Chimie de Coordination, ERA 670 CNRS, Université Louis Pasteur, F-67070 Strasbourg Cedex, France, Institut für Anorganische Chemie der Universität Würzburg, D-8700 Würzburg, FRG, and Laboratoire de Chimie Minérale, Ecole Nationale Supérieure de Chimie, F-67008 Strasbourg Cedex, France

# Synthesis and Spectroscopic Studies of Metal–Metal-Bonded Linear Heterotrimetallic Gold(I) Complexes. Crystal Structure of $[n\text{-}Bu_4N][Au[Cr(CO)_3\text{-}\eta\text{-}C_5H_5]_2]$

PIERRE BRAUNSTEIN,*† ULRICH SCHUBERT,‡ and MICHEL BURGARD§

*Received December 27, 1983*

A series of heterotrimetallic Au(I) anionic complexes of the general formula $[M'–Au–M']^-$ with M′ = $Mn(CO)_5$ (**1**), $Co(CO)_4$ (**2**), $Cr(CO)_3Cp$ (**3**), $Mo(CO)_3Cp$ (**4**), $W(CO)_3Cp$ (**5**), and $Fe(CO)_2Cp$ (**6**) have been prepared and characterized. The linear coordination about the gold atom is evidenced by infrared spectroscopy, particularly in the metal–metal stretching region where a strong absorption between 150 and 200 cm$^{-1}$ is typical for the $\nu_{as}$(Au–M′) vibration. The corresponding approximate force constants are compared with those of other related linear trimetallic complexes. It is found that metal–metal bond strength increases in the M′–M–M′ systems in the following sequence of M = Pd < Pt < Au < Hg. The same trend is observed for the covalency of these complexes as deduced from their $\nu$(CO) frequencies. The molecular structure of $[n\text{-}Bu_4N][Au[Cr(CO)_3Cp]_2]$ (**3**) has been determined by X-ray diffraction: $P2_1/c$ with $a$ = 1110.6 (6) pm, $b$ = 1690.5 (14) pm, $c$ = 2209.2 (8) pm, $\beta$ = 122.46 (3)°, and $Z$ = 4. The complex anion has approximate $C_2$ symmetry. The Cr(1)–Au–Cr(2) angle is 162.2 (3)°, and the Au–Cr distances are 264.1 (9) and 263.5 (8) pm. The coordination about the Cr atoms is of the "four-legged piano-stool" type. The $^{197}$Au Mössbauer parameters of **1**, **4**, and **6** have been measured and are compared with those obtained for $AuCl_2^-$ and $AuI_2^-$. Considering the linearity of these molecules, the IS and QS values are consistent with complexes in which the Au(I) center has a $sp_z$ hybridization. They furthermore confirm the bonding scheme deduced from infrared spectroscopy, in which $\sigma$ bonding between the metals is predominant and $\pi$ effects will arise from $\pi$ donation into the gold $6p_x$ and $6p_y$ orbitals.

## Introduction

Polymetallic complexes in which the metal atoms are connected to each other through metal–metal bonds only form now a well-known class in organometallic chemistry.[1,2] Previously, we have shown that the reaction of carbonylmetalates, $[M']^-$ with cis or trans square-planar palladium or platinum halide complexes can be successfully applied to the synthesis of heterotrimetallic chain complexes (eq 1).[3-7]

Such complexes are of interest for numerous reasons:

(i) They contribute to a better knowledge of the role of metal–metal bonding in stabilizing polymetallic complexes

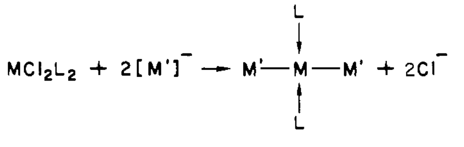

$$MCl_2L_2 + 2[M']^- \longrightarrow M'—\overset{\overset{L}{\downarrow}}{\underset{\underset{L}{\uparrow}}{M}}—M' + 2Cl^- \qquad (1)$$

M = Pd, Pt; L = py[3], RNC,[4,5] RCN,[6] CO;[6,7] M′ = $Mn(CO)_5$, $Co(CO)_4$, $Fe(CO)_3NO$, $Cr(CO)_3Cp$, $Mo(CO)_3Cp$, $W(CO)_3Cp$ ($Cp = \eta\text{-}C_5H_5$)

since, in these examples, their cohesion is achieved without the assistance of bridging ligands. This proved to be partic-

---

† Université Louis Pasteur.

‡ Universität Würzburg.

§ Ecole Nationale Supérieure de Chimie.

(1) Cotton, F. A.; Wilkinson, G. "Advanced Inorganic Chemistry", 4th ed.; Wiley-Interscience: New York, 1980.

(2) Roberts, D. A.; Geoffroy, G. L. In "Comprehensive Organometallic Chemistry"; Wilkinson, G., Stone, F. G. A., Abel, E. W., Eds.; Pergamon Press: Oxford, 1982; Chapter 40.

0020-1669/84/1323-4057$01.50/0